Inorganic Nanotubes

DOI: 10.1002/anie.200803447

Core–Shell PbI_2@WS_2 Inorganic Nanotubes from Capillary Wetting**

*Ronen Kreizman, Sung You Hong, Jeremy Sloan, Ronit Popovitz-Biro, Ana Albu-Yaron, Gerard Tobias, Belén Ballesteros, Benjamin G. Davis, Malcolm L. H. Green, and Reshef Tenne**

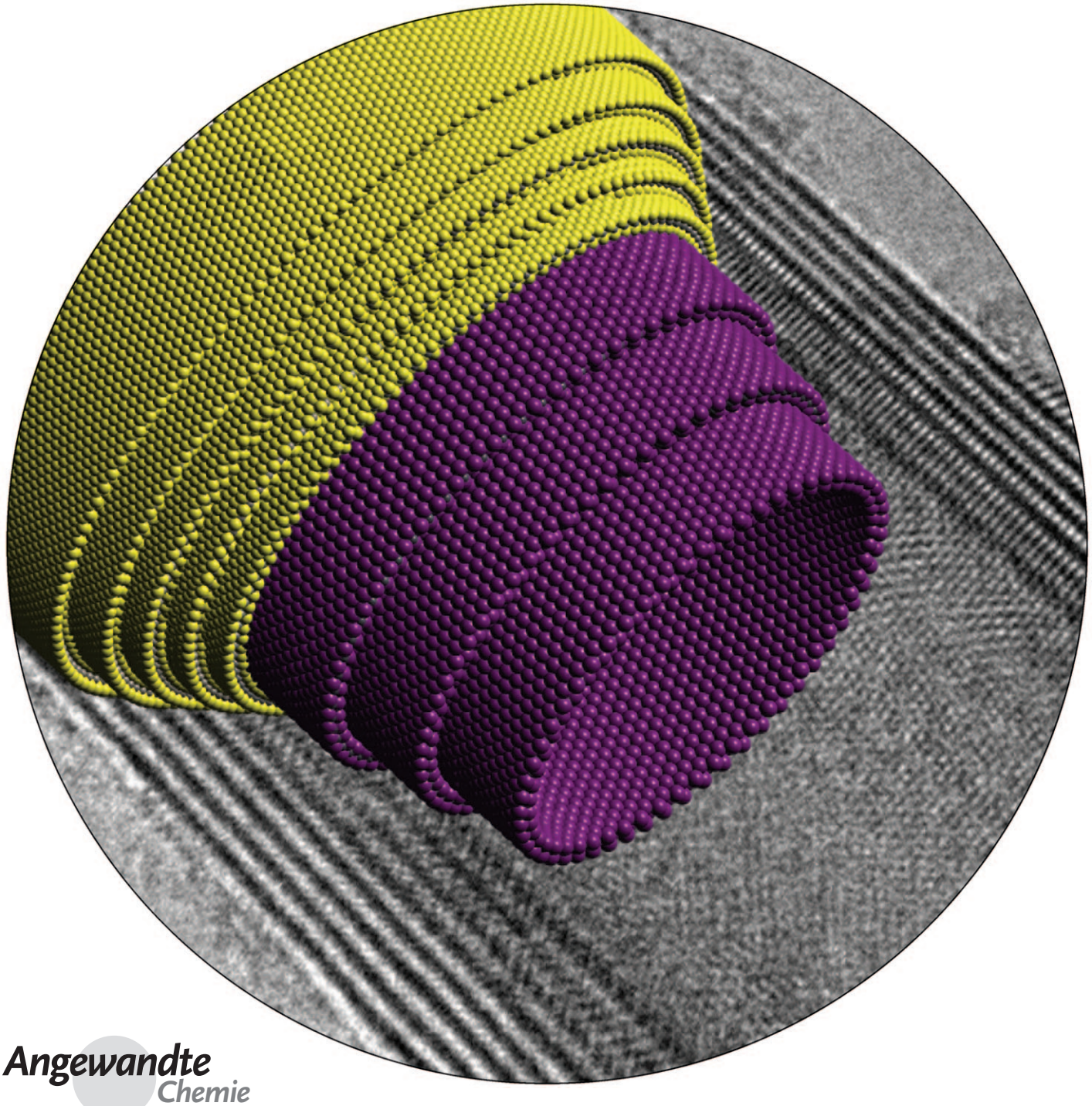

One of the defining structural features of nanotubular structures is their long inner hollow cavity. Capillarity has been shown to drive the wetting and filling of multiwalled carbon nanotubes (MWNTs) with liquid and molten-phase inorganic salts if the surface tension of the filling materials is less than about 180 $mN\,m^{-1}$.[1–2] It was subsequently shown that various inorganic salts can be encapsulated inside the comparatively narrow (0.8–1.5 nm) hollow core of single-walled carbon nanotubes (SWNTs) by molten-phase capillary wetting.[3] Salt encapsulation was shown to result in a profound change in the structural chemistry of the included material relative to its bulk form. In the case of salts such as KI, lowering of coordination without an overall change in structure was observed.[4] In other instances, a complete change in the structural chemistry was shown to occur, for example, for BaI_2[5] and CoI_2[6] crystallized in narrow SWNT capillaries. Here we demonstrate a new synthetic strategy allowing formation of core–shell nanotubular structures by using multiwall WS_2 nanotubes[7] as host templates. The relatively large diameter of the WS_2 nanotube (inner and outer diameters of about 10 and 20 nm, respectively) allows conformal folding of the guest PbI_2 layers on the interior wall of the WS_2 nanotube template, and thus leads to defect-free core–shell inorganic nanotubular structures that were not previously observed to form in MWNTs or SWNTs.

Transition metal dichalcogenides MS_2 (M = Mo, W) are among numerous inorganic compounds having layered structures. Each metal atom is coordinated by six sulfur atoms in a trigonal-prismatic fashion resulting in *aba*-type stacking within an individual MS_2 layer. Both graphite and MS_2 structures belong to the same $P6_3/mmc$ space group. This structural analogy suggested that closed polyhedra may also exist for the latter compounds.[7] Nanoparticles of various inorganic layered compounds, including WS_2,[7] MoS_2,[8] $NiCl_2$,[9] and SnS_2/SnS,[10] were shown to form tubular structures. For WS_2 nanotubes, the average inner diameters are in the range 10–12 nm, and the tips of as-formed tubules are mostly open-ended, so the structure is suitable for capillary filling. PbI_2 is a nonhygroscopic metal halide which adopts the layered CdI_2 structural archetype, while it also exhibits extensive twinning and polytypism. Within an individual PbI_2 two-dimensional (2D) layer, the stacking is *abc* rather than *aba*, as for WS_2 (see above). Several ordered polytypes of PbI_2 exist, of which the 2H, 4H, and 12R forms are most common. The polytype 2H PbI_2 ($a = 0.45580$, $c = 0.6986$ nm) is known to undergo a reversible phase transition: 2H to 4H or 12R in the temperature range 273–423 K.[11,12]

Multiwall (4–10 layers) WS_2 nanotubes were synthesized in a fluidized-bed reactor according to a previously published procedure.[7b] The phase containing WS_2 nanotubes was inserted into a quartz ampoule together with PbI_2. The quartz ampoules were placed in a furnace heated to 500 °C for periods of time ranging from several hours up to one month. After cooling, the samples were examined by high-resolution transmission electron microscopy (HRTEM), energy-dispersive X-ray spectroscopy (EDS), electron diffraction (ED), *Z*-contrast scanning transmission electron microscopy (STEM), and electron energy-loss spectroscopy (EELS). The HRTEM images and the corresponding details were obtained close to ideal Scherzer imaging conditions. Simulations of HRTEM images were performed by using a standard multislice algorithm and utilizing parameters representative of our instrument ($C_s = 0.6$ mm, accelerating voltage 300 kV).

The majority of the WS_2 nanotubes were found to be filled after annealing for one month. The PbI_2 filling mostly showed unique behavior inside the WS_2 nanotubes: formation of inner PbI_2 inorganic nanotubes inside WS_2 nanotube templates. Figure 1 shows a typical HRTEM image of a portion of the core–shell PbI_2@WS_2 nanotube, in which the encapsulated PbI_2 layers conformably cover the inner core of the host nanotubes. Longer annealing periods (two weeks to one month) lead to more perfect conformal coating of the WS_2 template by the inner PbI_2 nanotubes. The encapsulated PbI_2 inside WS_2 nanotubes showed, in addition to the nanotubular structure, both amorphous and nontubular crystalline filling (see Supporting Information).

The HRTEM image contrast of the WS_2 nanotubes was apparently more intense than that of the heavier PbI_2 inner nanotubes, although the latter displayed more complex contrast (see Figure 1c). This observation can be attributed to the larger atomic-number difference between the W ($Z = 74$) and S ($Z = 16$) layers versus the Pb ($Z = 82$) and I ($Z = 53$) layers. In the obtained images, the layers of W atoms appear much darker than the corresponding layers of S atoms. In the PbI_2 layers, however, the contrast is more evenly distributed between Pb and I layers due to their more similar atomic numbers. Image simulations based on a model of concentric W, S, Pb, and I shells with the same arrangement as we predict for our composite (Figure 1c, right) reproduce the obtained contrast reasonably well. Another possible contribution to the differential contrast of the PbI_2 nanotubes is the reduced occupancy of the 2D PbI_2 shells. In PbI_2, density measurements revealed an occupancy of about 80–85% when

[*] R. Kreizman,[+] Dr. R. Popovitz-Biro, Dr. A. Albu-Yaron, Prof. R. Tenne
Department of Materials and Interfaces
Weizmann Institute of Science
Rehovot 76100 (Israel)
Fax: (+972) 8-934-4138
E-mail: tenne@weizmann.ac.il

S. Y. Hong,[+] Dr. G. Tobias, Dr. B. Ballesteros, Prof. B. G. Davis, Prof. M. L. H. Green
Department of Chemistry
University of Oxford
Oxford OX1 3TA (UK)

Dr. J. Sloan[++]
Department of Engineering and Materials
Queen Mary, University of London
London E1 4NS (UK)

[++] current address: School of Physics, University of Warwick (UK)

[+] These authors contributed equally to this work.

[**] We thank Dr. Rita Rosentsveig for synthesis of the WS_2 nanotubes. This work was supported by the G. M. J. Schmidt Minerva Center, the Harold Perlman Fund, the Gurwin Fund, the Irving and Cherna Moskowitz Center for Nano and Bio-Nano imaging, and the Israel Science Foundation. J.S. acknowledges the Royal Society for a University Research Fellowship and G.T. acknowledges FP6 Marie Curie IEF MEIF-CT-2006-024542.

Supporting information for this article is available on the WWW under http://dx.doi.org/10.1002/anie.200803447.

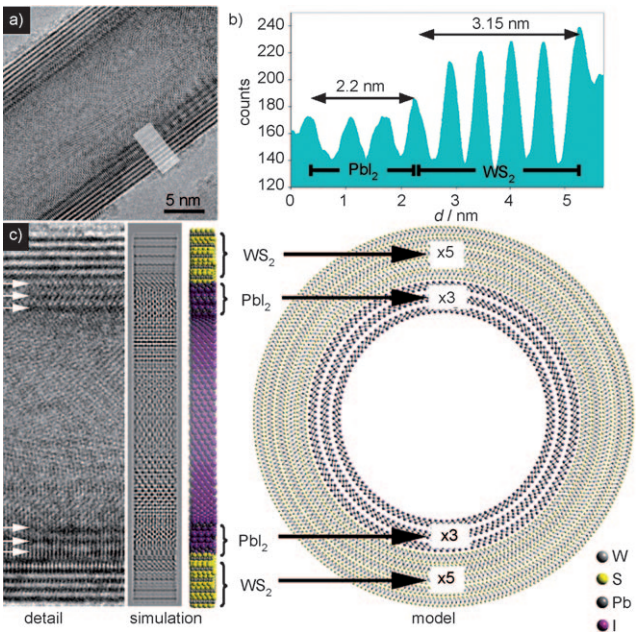

Figure 1. a) HRTEM micrograph showing a core–shell PbI_2@WS_2 composite nanotube. b) Line profile obtained from the indicated region in (a) showing two types of nanotube layers: five outer WS_2 layers with sharper contrast and an average spacing of 0.63 nm and three inner layers with more complex contrast and an average spacing of 0.73 nm, corresponding to three concentric PbI_2 nanotubes. c) Detail from (a) showing the complex contrast of the inner PbI_2 layers (arrowed) relative to the outer WS_2 layers. To the right of the detail is a simulation and a cutaway space-filling model (left) and cross-sectional structure model (right) with both WS_2 (*aba* stacking) and PbI_2 layers (*abc* stacking) indicated.

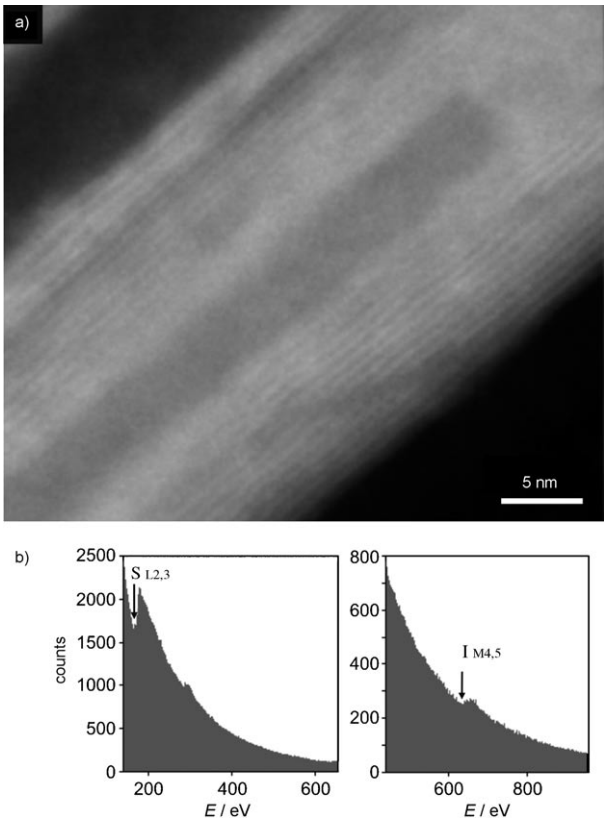

Figure 2. a) *Z*-contrast dark-field STEM image of a core–shell PbI_2@WS_2 nanotube. b) EELS analysis of the core–shell structure showing both S $L_{2,3}$ and I $M_{4,5}$ edges.

compared to crystallographic calculations (i.e., 5.0 $g\,cm^{-3}$ versus a theoretical density of 6.09 $g\,cm^{-3}$).[11a]

The EELS and EDS analyses complementarily confirmed the presence of W, S, Pb, and I as constituting elements of the core–shell inorganic nanotubes. The EELS spectrum revealed both the S $L_{2,3}$ and I $M_{4,5}$ edges (Figure 2b). In EDS analysis, the $S_{K\alpha}$ and $Pb_{M\alpha}$ peaks overlap, but the $Pb_{L\alpha}$ peak is clearly visible (Figure 3). Since the inner diameter of the WS_2 nanotube template is relatively constant, the number of PbI_2 layers in these core–shell structures is limited to about 3–5. The typical length of the inner PbI_2 nanotubes did not exceed a few 100 nm, and the smallest diameter of inner PbI_2 nanotubes was found to be about 3 nm.

Imaging with *Z*-contrast (Figure 2a) was further used to determine the presence of the core–shell PbI_2@WS_2 structures. A *Z*-contrast image is formed in a STEM by focusing an electron probe on the specimen and detecting electrons that scatter out to an annular dark-field detector. It is an incoherent mode that uses Rutherford scattering to form *Z*-contrast images in which the intensity scales with the square of the atomic number. This results in a gradual increase of contrast from outer layers of WS_2 to inner layers of PbI_2, though it may also be affected by actual crystallographic densities and the relative numbers of both types of layers.[13] In Figure 2a a PbI_2 meniscus is observed at the top-right corner of the image with high contrast, from where the PbI_2 tubular structure is formed. This phenomenon was also observed by HRTEM (see Supporting Information).

Encapsulated inorganic salts adopt different crystal structures from those in bulk form depending on the diameter of the host carbon nanotubes. This was attributed to the reduced coordination of the surface atoms of the crystals and the close

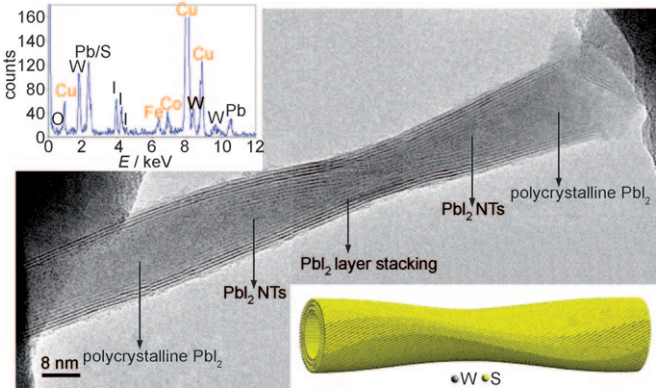

Figure 3. HRTEM image constructed from a series of HRTEM images obtained along the length of the nanotube. The EDS spectrum (top inset) shows signals due to W, S, Pb, and I which can be attributed to the core–shell-type inorganic nanotube. Other indicated signals (O, Cu, Fe, and Co) correspond either to background signals not attributable to the specimen or to contamination. A conceptual model for the twisted outer WS_2 nanotube is also shown (bottom inset).

proximity of the van der Waals surface of the confining nanotube.[4] There is also experimental evidence of a strong interaction between the encapsulated material and the encapsulating SWNT, as evidenced by twisted 1D crystals of CoI_2 formed in narrow SWNTs.[6] Figure 3 shows how the interaction of guest lattice and host WS_2 nanotube lattice depends on strain. The total energy of a tubular structure is higher than that of infinite layers due to the bending energy. However, the tubular structure can be energetically favored over finite layers due to elimination dangling bonds at the rim. The van der Waals interaction is known to lower the total energy of multiwall nanotubes.[14] The calculated strain energies for the inorganic nanotubes follow a $1/R^2$ behavior, where R is the radius of the tube. Thus, the strain energy of MoS_2 nanotubes varies according to $1/R^2$ and is one order of magnitude larger than that of carbon nanotubes with similar diameters.[14] The PbI_2 nanotubes are expected to show a similar dependence of the elastic energy on radius, and consequently they cannot be formed inside nanotube cores smaller than say 3 nm. As shown in Figure 3, encapsulated PbI_2 lattices show crystallographic changes [polycrystalline↔nanotubular structure↔multilayer stacking]. The most twisted (strained) part apparently shows multilayer stacking, whereas a nanotubular structure starts to form as the strain is released. So far only nanotubular structures PbI_2 have been observed to form inside host WS_2 nanotubes, and we have not observed "free" inorganic fullerene-like (IF) PbI_2 structures such as have been reported for other materials.[7–10]

In summary, we have reported the molten-phase wetting behavior of PbI_2 within WS_2 nanotube capillaries. In addition to one-dimensional PbI_2 crystals occluded inside the host nanotubes, core–shell PbI_2@WS_2 inorganic nanotubes were observed. Moreover, image simulation after structural modeling showed good agreement with the experimental HRTEM image, and thus further confirmed this core–shell structure. We hope that this study can be the starting point for many more inorganic core–shell nanotubes in which various layered compounds are templated both within and atop host tubules. Using a different approach, we have also prepared WS_2@MoS_2 core–shell nanotubes (to be published elsewhere). This kind of reaction could lead to new materials for passive protection of organs against ionizing irradiation, as well as for nanosensors for ionizing radiation.

Experimental Section

Optimized reaction conditions: A mixture of multiwall WS_2 nanotubes, IF-WS_2 nanoparticles (30 mg), and PbI_2 (120 mg, Alfa Aesar, 98.5%, m.p. 402°C) were ground with a mortar and pestle and transferred to a silica quartz ampoule. Crystalline iodine (ca. 15 mg, Alpha Aesar, 99.5%) was then added to the ampoule. After pumping to high vacuum (ca. 10^{-5} mbar) and sealing, the ampoule was inserted in a preheated furnace, where it dwelled at 500°C for 30 d before slow overnight cooling to room temperature.

The product was sonicated in ethanol, placed on a carbon/collodion-coated Cu grid, and analyzed by TEM (Philips CM-120, 120 kV), STEM (JEOL JEM-3000F field-emission gun, 300 kV, low-pass Butterworth filter), and HRTEM (FEI Tecnai F-30 with EELS or JEOL JEM-3000F field-emission gun, 300 kV). Images were acquired digitally on a Gatan model 794 (1k × 1k) CCD camera, the magnification of which was calibrated with Si[110] lattice spacing. EDS was performed with an electron probe 0.5 nm in diameter.

Received: July 16, 2008
Published online: November 21, 2008
Publication delayed at author's request

Keywords: chalcogenides · core–shell materials · nanostructures · nanotubes · template synthesis

[1] a) P. M. Ajayan, S. Iijima, *Nature* **1993**, *361*, 333–334; b) S. C. Tsang, Y. K. Chen, P. J. F. Harris, M. L. H. Green, *Nature* **1994**, *372*, 159–162.
[2] a) E. Dujardin, T. W. Ebbesen, H. Hiura, K. Tanigaki, *Science* **1994**, *265*, 1850–1852; b) M. R. Pederson, J. Q. Broughton, *Phys. Rev. Lett.* **1992**, *69*, 2689–2692; c) J. Y. Chen, A. Kutana, C. P. Collier, K. P. Giapis, *Science* **2005**, *310*, 1480–1483.
[3] For a review see: a) J. Sloan, A. I. Kirkland, J. L. Hutchison, M. L. H. Green, *Chem. Commun.* **2002**, 1319–1332; b) J. Sloan, A. I. Kirkland, J. L. Hutchison, M. L. H. Green, *Acc. Chem. Res.* **2002**, *35*, 1054–1062.
[4] R. R. Meyer, J. Sloan, R. E. Dunin-Borkowski, A. I. Kirkland, M. C. Novotny, S. R. Bailey, J. L. Hutchison, M. L. H. Green, *Science* **2000**, *289*, 1324–1326.
[5] J. Sloan, S. J. Grosvenor, S. Friedrichs, A. I. Kirkland, J. L. Hutchison, M. L. H. Green, *Angew. Chem.* **2002**, *114*, 1204–1207; *Angew. Chem. Int. Ed.* **2002**, *41*, 1156–1159.
[6] E. Philp, J. Sloan, A. I. Kirkland, R. R. Meyer, S. Friedrichs, J. L. Hutchison, M. L. H. Green, *Nat. Mater.* **2003**, *2*, 788–791.
[7] a) R. Tenne, L. Margulis, M. Genut, G. Hodes, *Nature* **1992**, *360*, 444–446; b) R. Rosentsveig, A. Margolin, Y. Feldman, R. Popovitz-Biro, R. Tenne, *Chem. Mater.* **2002**, *14*, 471–473; c) I. Kaplan-Ashiri, S. R. Cohen, K. Gartsman, V. Ivanovskaya, T. Heine, G. Seifert, I. Wiesel, H. D. Wagner, R. Tenne, *Proc. Natl. Acad. Sci. USA* **2006**, *103*, 523–528; d) For a review, see: R. Tenne, *Nat. Nanotechnol.* **2006**, *1*, 103–111.
[8] a) L. Margulis, G. Salitra, R. Tenne, M. Tallanker, *Nature* **1993**, *365*, 113–114; b) Y. Feldman, E. Wasserman, D. J. Srolovitz, R. Tenne, *Science* **1995**, *267*, 222–225.
[9] a) Y. R. Hacohen, E. Grunbaum, R. Tenne, J. Sloan, J. L. Hutchison, *Nature* **1998**, *395*, 336–337; b) Y. R. Hacohen, R. Popovitz-Biro, E. Grunbaum, Y. Prior, R. Tenne, *Adv. Mater.* **2002**, *14*, 1075–1078.
[10] S. Y. Hong, R. Popovitz-Biro, Y. Prior, R. Tenne, *J. Am. Chem. Soc.* **2003**, *125*, 10470–10474.
[11] a) B. Palosz, W. Steurer, H. Schulz, *J. Phys. Condens. Matter* **1990**, *2*, 5285–5295; b) E. Salje, B. Palosz, B. Wruck, *J. Phys. C* **1987**, *20*, 4077–4096.
[12] E. Flahaut, J. Sloan, S. Friedrichs, A. I. Kirkland, K. S. Coleman, V. C. Williams, N. Hanson, J. L. Hutchison, M. L. H. Green, *Chem. Mater.* **2006**, *18*, 2059–2069.
[13] a) P. D. Nellist, S. J. Pennycook, *Science* **1996**, *274*, 413–413; b) X. Fan, E. C. Dickey, P. C. Eklund, K. A. Williams, L. Grigorian, R. Buczko, S. T. Pantelides, S. J. Pennycook, *Phys. Rev. Lett.* **2000**, *84*, 4621–4624; c) D. E. Jesson, S. J. Pennycook, *Proc. R. Soc. London Ser. A* **1995**, *449*, 273–293; d) S. Y. Hong, G. Tobias, B. Ballesteros, F. El Oualid, J. C. Errey, K. J. Doores, A. I. Kirkland, P. D. Nellist, M. L. H. Green, B. G. Davis, *J. Am. Chem. Soc.* **2007**, *129*, 10966–10967.
[14] a) G. Seifert, T. Kohler, R, Tenne, *J. Phys. Chem. B* **2002**, *106*, 2497–2501; b) G. Seifert, H. Terrones, M. Terrones, G. Jungnickel, T. Frauenheim, *Phys. Rev. Lett.* **2000**, *85*, 146–149.

